International Journal of Engineering, Mathematical and Physical Sciences
ISSN: 2517-9934
Vol:3, No:10, 2009

CFD simulation of Pressure Drops in Liquid Acquisition Device Channel with Sub-Cooled Oxygen

David J. Chato, John B. McQuillen, Brian J. Motil, David F. Chao, and Nengli Zhang

***Abstract*—** In order to better understand the performance of screen channel liquid acquisition devices (LADs) in liquid oxygen (LOX), a computational fluid dynamics (CFD) simulation of LOX passing through a LAD screen channel was conducted. In the simulation, the screen is taken as a 'porous jump' where the pressure drop across the screen depends on the incoming velocity and is formulated by $\Delta p = Av + Bv^2$. The CFD simulation reveals the importance of the pressure losses due to the flow entering from across the screen and impacting and merging with the channel flow and the vortices in the channel to the cumulative flow resistance. In fact, both the flow resistance of flows impact and mergence and the resistance created by vortices are much larger than the friction and dynamic pressure losses in the channel and are comparable to the flow resistance across the screen. Therefore, these resistances in the channel must be considered as part of the evaluation for the LAD channel performance. For proper operation of a LAD in LOX these resistances must be less than the bubble point pressure for the screen channel in LOX. The simulation also presents the pressure and velocity distributions within the LAD screen channel, expanding the understanding of the fluid flow characteristics within the channel.

***Keywords*—** Liquid acquisition devices, liquid oxygen, pressure drop, vortex, bubble point, flow rate limitation.

I. Introduction

In future space vehicles, cryogenic propellants are usually transported from their storage tanks to an engine in liquid state. This is easily accomplished on earth using gravity provided that the tank outlet is placed at the bottom. Under the effect of earth gravity, buoyancy effectively separates the gas/vapor and liquid in the tank and prevents the gas/vapor mixing into the liquid propellants in the transport channels. However, the acceleration forces and difficult thermal environment conditions in space complicate the storage and transport of propellants, especially with regards to separating of the gas/vapor and liquid. In low gravity or reduced acceleration environments in space missions, surface tension, rather than buoyancy, becomes dominant in determining the relative positions of liquid and vapor propellants during quiescent or coast periods. During the high acceleration engine thrust period, single-phase liquid is delivered from the tank simply by "draining" the liquid from the tank "bottom" and using an anti-vortex baffle over the tank outlet to minimize gas/vapor ingestion due to the flow swirl. In other flight periods of space vehicles, single-phase liquid withdrawal is a challenge in low gravity because liquid may not cover the tank outlet. Consequently, the investigation of the performance of surface tension propellant acquisition/expulsion devices has been a critical research and development concern for space missions. Many types of these devices have been built, tested and used for hypergolic propellants, such as nitrogen tetroxide (N_2O_4) and monomethyl hydrazine (MMH), but development for cryogenic propellants has been lagging. These devices are designed to achieve a unique set of performance requirements under appropriate environmental conditions; there is no universal design that satisfies all mission criteria for all applications [1]. Future space vehicles require using non-toxic, cryogenic propellants, not only stemming from the offering of performance advantages over the toxic hypergolic propellants but also from environmental and handling concerns [2]. For cryogenic propellants, the "settling" method previously used to position propellants over the tank outlet will have to be relinquished, due to conflicting vehicle requirements. A capillary flow liquid acquisition device (LAD) is required for propellant management [3].

Capillary flow LADs have been well characterized for storable toxic propellants [2], [4], but there are only a few LAD experiments and data for cryogenic propellants, especially with liquid oxygen (LOX). Kudlac and Jurns [2] made the first known non-proprietary effort to measure bubble point and to collect LAD data in LOX. Jurns and McQuillen [5] extended the range of LOX fluid conditions examined, by reporting on bubble point testing with sub-cooled LOX, and provided insight into factors that may predict LAD bubble point pressures. Limited by the measuring technologies, the detailed pressure and velocity distributions in the LAD channel have been unknown. Computational fluid dynamics (CFD) simulation can provide this essential information, thus leading to a better understand LAD screen channel

David J. Chato is with NASA Glenn Research Center, Cleveland, OH 44135 USA (e-mail: david.j.chato@nasa.gov).
John B. McQuillen is with NASA Glenn Research Center, Cleveland, OH 44135 USA (e-mail: john.b.mcquillen@nasa.gov).
Brian J. Motil is with NASA Glenn Research Center, Cleveland, OH 44135 USA (e-mail: brian.j.motil@nasa.gov).
David F. Chao is with NASA Glenn Research Center, Cleveland, OH 44135 USA (e-mail: david.f.chao@nasa.gov).
Nengli Zhang is with Ohio Aerospace Institute at NASA Glenn Research Center, Cleveland, OH 44135 USA (corresponding author to provide phone: 216-433-8750; fax: 216-433-8050; e-mail: nengli.zhang@grc.nasa.gov).

performance for LOX.

II. CFD MODEL OF LAD CHANNEL

Under NASA's continuing Cryogenic Fluid Management (CFM) development program, tests will be conducted in a prototypical screen channel LAD using LOX at flow rates representative of those for the main engine for the Lunar Stage Ascent Module. This screen channel LAD is shown in Fig. 1. A screen of Dutch Twill mesh 200x1400 is welded along the top rim of the LAD channel. Surface tension and the small pore openings in the screen mesh prevent gas/vapor from passing through the screen while allowing liquid to pass freely. The plate is positioned above the screen mesh to simulate the tank wall. This cover plate provides additional protection from gas/vapor penetration into the LAD channel and is a source of additional flow resistance. A detail of the screen is shown in Fig. 2. The CFD simulation model is identical with the test assembly. GAMBIT™ was used to create the computational grid mesh and FLUENT™ 6.3.26 performed the simulation.

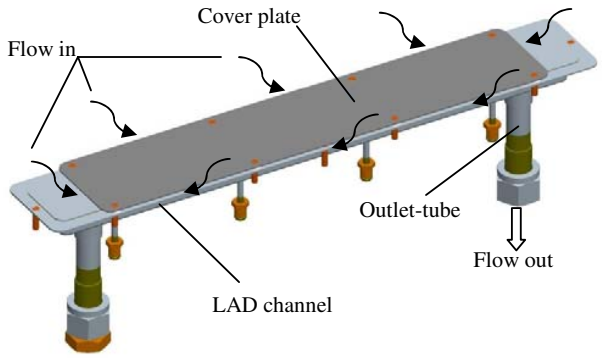

a) Test LAD channel assembly with cover plate

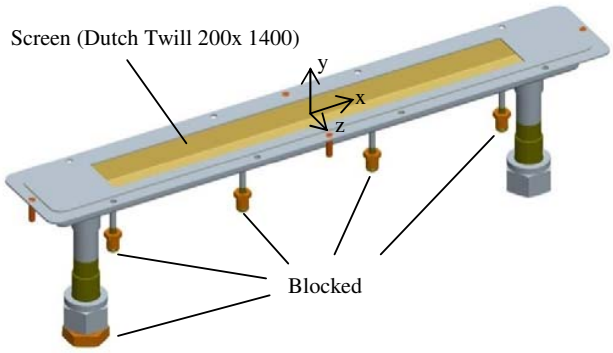

b) Test LAD channel assembly without cover plate

Fig. 1 Test LAD channel assembly

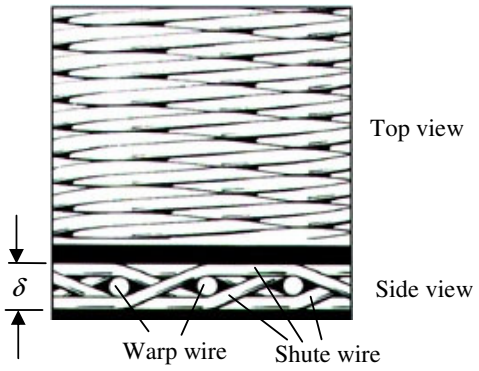

Fig. 2 Dutch Twill mesh screen weaving pattern

The basic geometry of the LAD channel is follows. The flow channel is 609.6 mm (24 in) long by 50.8 mm (2 in) wide by 25.4 mm (1 in) deep. A lip along the top of the channel facilitates attachment of the screen section to the channel and forms a screen window of 482.6 mm (19 in) long by 50.8 mm (2 in) wide. The outlet-tube has an inner diameter of 23.622 mm (0.93 in). The origin of coordinates was set at the center of screen top surface, as shown in Fig. 1b. Since the screen is too thin (the screen thickness $\delta \approx 0.15$ mm) to create the grid mesh, the screen is treated as a 'porous-jump' whose parameters determined by the screen characteristics.

Based on the experimental data with liquid nitrogen, Armour and Cannon [6] developed a general correlation of screen friction factor which is applicable to the flow through all types of woven metal screens:

$$f = a/Re + b \tag{1}$$

where $f = \Delta p \varepsilon^2 D/(Q\delta\rho V^2)$, $Re = \rho V/(\mu s^2 D)$, $a = 8.61$ *and* $b = 0.52$. Δp is the pressure drop for fluid flow through the screen, while the parameters Q, ε, D, δ, and s are the tortuosity factor, the void fraction, the pore diameter, the screen thickness, and the surface area to unit volume ratio, respectively, while ρ, μ, and V are the density, viscosity, and incoming velocity of the fluid passing through the screen, respectively. The parameters, Q, ε, D, δ, and s were determined by Armour and Canon based on their analysis and measurements for each specified screen. In fact, (1) can be directly written as

$$\Delta p = AV + BV^2 \tag{2}$$

where $A = 8.61Q\delta\mu s^2/\varepsilon^2$; $B = 0.52Q\delta\rho/\varepsilon^2 D$.

Using Armour and Cannon's data and experimental results for liquid hydrogen, Cady [7] found that the constants $a = 8.61$ and $b = 0.52$ in (1) provide good agreement for the screen of Plain Dutch mesh 24x110, while considerable errors occur in other screens. He revised (1) with different values of a and b for each specified screen. For the screen of 200x1400 Dutch Twill mesh, $a = 4.2$ and $b = 0.20$, while $Q = 1.3$, $\varepsilon = 0.248$, $D = 0.000010$ m, $\delta = 0.0001524$ m, $s = 65390$ 1/m.

Consequently, two major parameters for the porous-jump in

FLUENT, the face permeability α and the pressure jump coefficient C, were defined and determined as follows.

$$\alpha = \mu\delta/A = \varepsilon^2/(aQs^2) = 2.634438\text{x}10^{-12}\ \text{m}^2 \quad (3)$$

$$C = 2B/\rho\delta = 2bQ/(\varepsilon^2 D) = 8.454735\text{x}10^{5}\ 1/\text{m} \quad (4)$$

Seven cases, each with a different working flow rate, were examined for sub-cooled LOX at a condition of 1620269 Pa (235 psi), 90 K to assess the LAD channel performance and reveal pressure and velocity distribution within the channel.

III. CFD SIMULATION RESULTS

The CFD simulation results show that although both pressure drops across the screen and along the channel change with the working flow rates, the flow and pressure distribution patterns are the same for all cases. Typical flow pattern in the channel is shown in Fig. 3, while Fig 4 shows the corresponding pressure distribution pattern.

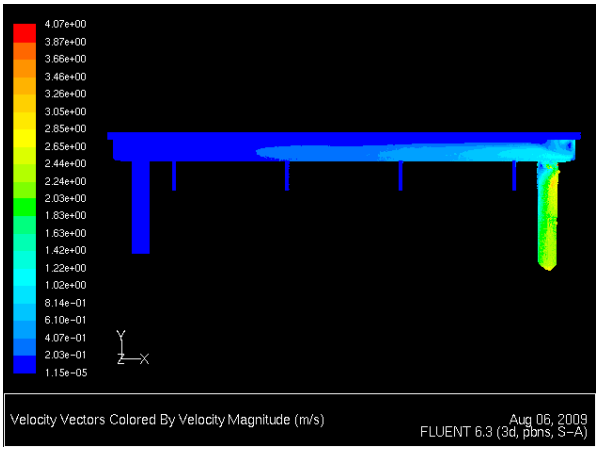

a) Velocity vectors distribution in the LAD channel.

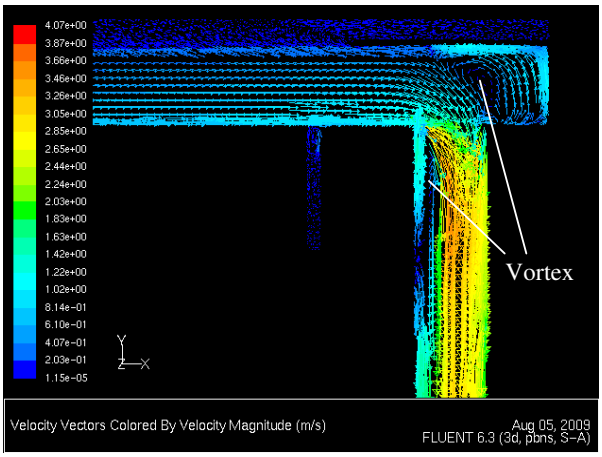

b) Magnified view of velocity vectors near the outlet tube at center section (z=0).

Fig 3 Velocity vectors in the LAD channel for the case of working flow rate 1.096 kg/s.

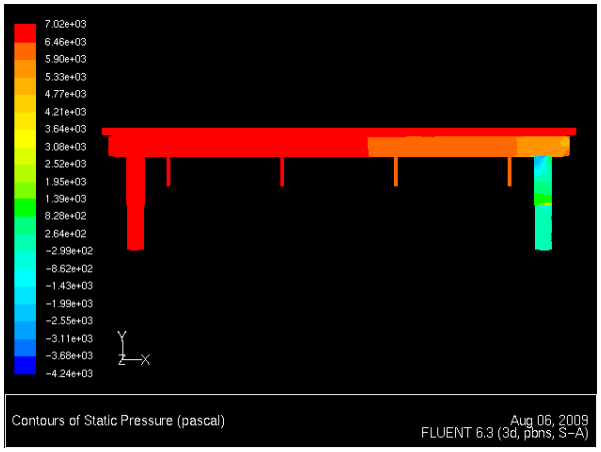

a) Pressure distribution in the LAD channel.

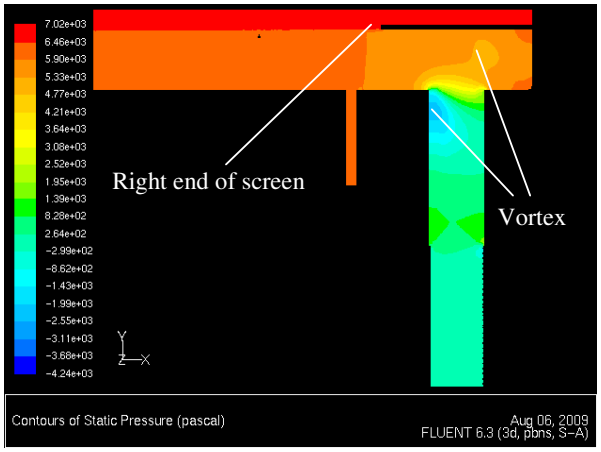

b) Magnified view of pressure distribution near the outlet tube at center section (z=0).

Fig.4 Pressure distribution in the LAD channel for the case of working flow rate 1.096 kg/s.

It can be seen that the LOX passing through the screen flows towards the outlet-tube. As the flow approaches the outlet-tube, the velocity increases due to the additional LOX flow entering the LAD channel. Two vortex zones occur in the vicinity of the outlet-tube entrance: The first zone is located at the right end of the channel while the other is located at the inner side of the outlet-tube under the entrance, as indicated in Figs. 3b and 4b. These vortices create local low pressure zones in these areas. Worthy of note is that the pressure drop across the screen increases along channel length because of the augmentation of flow rate along the channel length, resulting in larger flow resistance. As mentioned above, the pressure distribution patterns remain the same for all of the different working flow rates. Two typical pressure distributions along the channel length at different levels, just above the screen (y = 2 mm), just under the screen (y = - 3mm), and at the channel center line (y = -12.7 mm), are shown in Fig. 5. For the case of working flow rate G = 0.237 kg/s, the pressure drop across the

screen at the left end of the screen, far from the outlet-tube (x = - 241 mm), is Δp_{sl} = 90 Pa, while at the right end of the screen, close to the outlet-tube (x = 241 mm), the pressure drop across the screen Δp_{sr} = 127 Pa. For G = 1.488 kg/s, Δp_{sl} = 510 and Δp_{sr} = 2000 Pa.

In Fig. 5, the area between the vertical dotted lines corresponds to the channel length covered by the screen. The area beyond these dotted lines corresponds to the closed area of the channel. In the right closed area of the channel, there are no pressure losses from an increased LOX flow, and consequently, the pressure presents a short constant region followed by a sharp decrease because of the vortex. This is depicted in Fig. 5 with the annotation 'Just under screen'. Obviously, the vortex affects the pressure at the channel center more; therefore, no constant pressure region occurs at the channel center line. The vortex creates a low pressure zone in the channel that yields the largest pressure drop, Δp_{top}, at x = 282 mm along the channel center line. For G = 0.237 kg/s, Δp_{top} = 147 Pa, while for of G = 1.488 kg/s, Δp_{top} = 3250 Pa.

In fact, the lowest pressure in the entire LAD channel assembly occurs within the vortex in the outlet-tube. The step-change in the flow area at the entrance of the outlet-tube the vena-contracta effect to create a negative pressure zone. A produces a considerable large pressure loss that combines with typical pressure distribution curve in the LAD channel along the outlet-tube center line (y-axis direction) is shown in Fig. 6. For G =1.488 kg/s, the lowest pressure, -500 Pa, occurs at y = - 40 mm on the outlet-tube center line. That means the maximum pressure drop in the entire LAD channel assembly is 13500 Pa, much greater than the pressure drop of 3250 Pa within the channel alone.

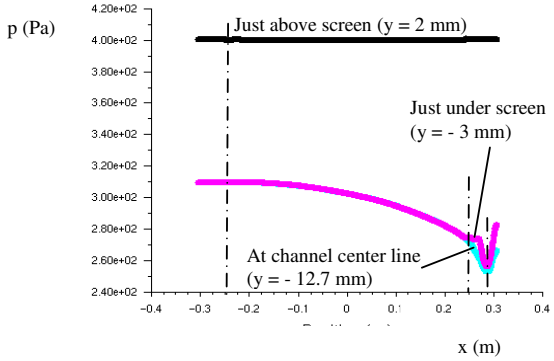

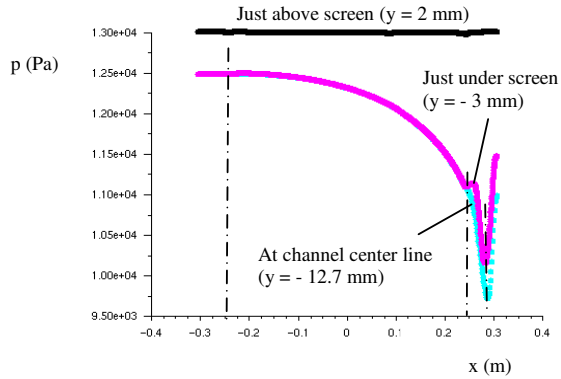

at different levels.

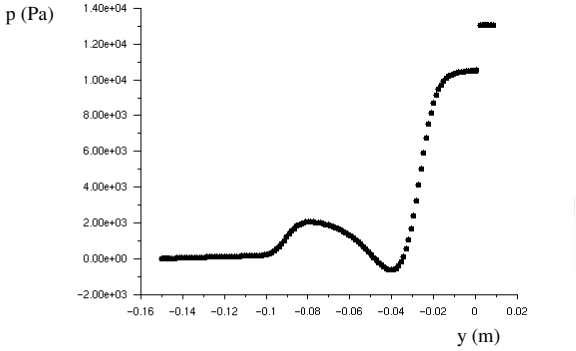

let-tube center length (y-axis
= 1.488 kg/s.

I. DISCUSSIONS

A. Flow Rate across Screen

The CFD simulations revealed that as LOX passes through the screen and flows toward the outlet-tube in the channel, the flow velocity and rate in the channel is continuously augment along the channel length, x-axis direction, as shown in Fig. 7. This continuous flow rate augmentation along the channel increases the flow resistance resulting in a continuous pressure drop along the channel. Consequently, the pressure drop across the screen increases along the channel length, resulting in a corresponding increase along the channel length in the flow rate passing through the screen.

Figure 8 shows the distributions of velocity flowing out of the screen for the cases of G = 1.096 kg/s and G = 0.237 kg/s. It can be seen that although the flow profiles are different for the different working flow rates, the general tendency of the local velocity passing through the screen is incremental along the channel length. In the left portion of the screen, far from the outlet tube, lower velocities occur along the edges and in the central region, while closer to the outlet-tube, the velocity in the middle reaches maximum and gradually decreases toward the edges.

Obviously, the position of the outlet-tube greatly affects the flow pattern of LOX passing through the screen. As it is seen in Figs. 1 and 4b, the outlet-tube is located at channel's right end and creates a very low pressure zone in the channel by the entrance of the outlet-tube, as seen in Figs. 4 and 5. Consequently, the local flow rate of LOX passing through the screen is significantly larger at the screen's right end,

especially along the screen centerline, as shown in Figs. 7 and 8.

B. Flow Resistance in the LAD Channel

Since the flow in the channel is continuously merging with flow from across the screen the flow is subjected to an increasing flow resistance along the channel. Obviously, this flow resistance is neither the simple frictional resistance nor the geometrical resistance created by change in the cross-sectional flow area. Both of these are usually ignored for their relatively small contributions. Previous investigators may have considered this as a frictional resistance. The flow resistance

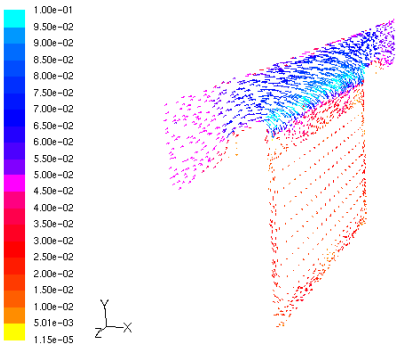

a) At leftmost end of screen (x = -0.24 m)

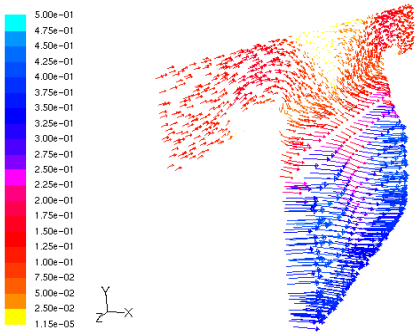

b) At middle of screen (x = 0.0 m)

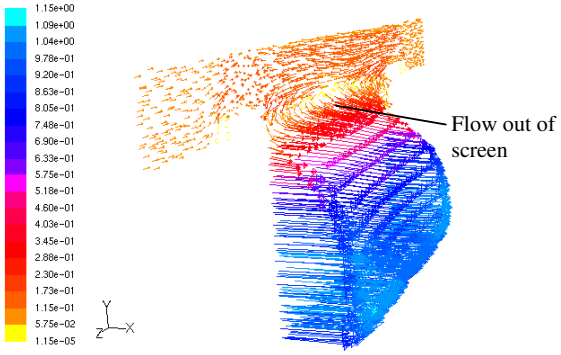

c) At rightmost end of screen (x = 0.24 m)

Fig. 7 Velocity vectors at different y-z sections for the case of G = 1.096 kg/s.

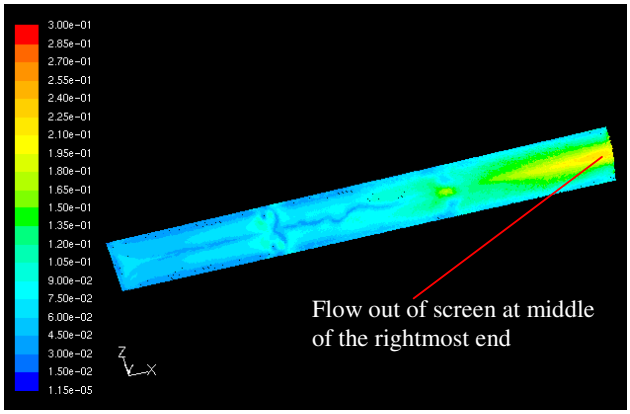

a) For the case of G = 1.096 kg/s

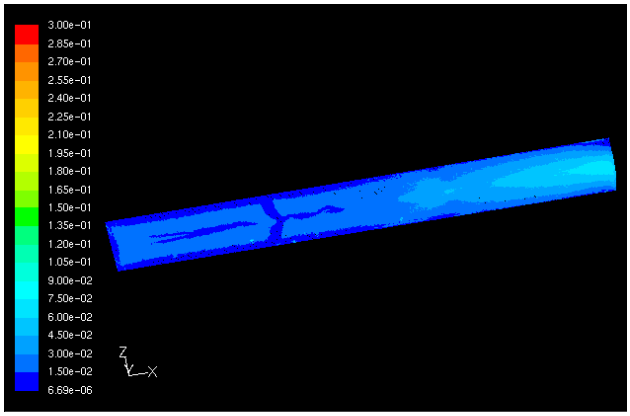

b) For the case of G = 0.237kg/s

Fig. 8 Velocity distribution on the screen surface facing to the channel for different cases of flow rates

produced by the impact of the flow entering from across the screen and the mergence with the flow in the channel, Δp_{im}, is relatively small for slow flow rates, but grows very rapidly with the working flow rate. For example, from Fig. 5, for G = 0.237 kg/s, $\Delta p_{im} = \Delta p_{sr} - \Delta p_{sl}$ = 37 Pa which is only 0.41times the pressure drop across the screen, i.e. Δp_{im} = 0.41 Δp_{sl}. However, for G = 1.488 kg/s, $\Delta p_{im} = \Delta p_{sr} - \Delta p_{sl}$ = 1490 Pa or 2.92 Δp_{sl}. The mathematical expression of the relationship between the resistance Δp_{im} and the working flow rate G has not been developed. More experimental and theory studies are needed.

C. Bubble Point Limitation

As it is well known, the total pressure loss in a LAD channel must be less than the bubble point pressure to prevent vapor ingestion into the LAD channel. According to the measurement results by Jurns and McQuillen [5], for the screen of Dutch Twill 200 x 1400 mesh, the average value of bubble points of LOX at 161.7 R (89.83 K) is 2500.8 Pa.

However, the experimental data ranged between 2115.1 to 2737.2 Pa. The limitation of the total pressure loss in the LAD channel should be put at the low end of the experimental data for the safe consideration, i.e. the limiting total pressure loss should be 2115 Pa.

Although this limitation is that the total pressure loss in the system must be less than the bubble point pressure, the pressure losses in the outlet-tube should be ruled out if the outlet-tube does not contribute towards the liquid acquisition through a screen-type construction. However, the pressure loss within the screen channel should be included. Three strategic pressure drops in the channel vs. the working flow rate are plotted in Fig. 9.

It can be seen that for the test LAD channel simulated here, when the working flow rate G > 1.22 kg/s (2.69 lb/s), the largest pressure drop in the channel would exceed the bubble point pressure. Thus, the performance of this LAD channel assembly is acceptable for flow rates less 1.22 kg/s. However, if the vortices at the outlet-tube can be eliminated by changing the position and alignment of the outlet-tube, the working flow rate limitation would increased to at least 1.577 kg/s. The simplest construction of the LAD channel assembly is to align the outlet-tube with the LAD channel length, as was in [2]. Furthermore, a gradual, smooth connection between the channel and the outlet-tube, such as a horn-type connection, can further reduce the size of the vortex zone. This may also improve the flow rate pattern of the flow passing through the screen. A more even flow rate distribution over the screen would decrease the flow resistance created by the flows impact and mergence. It should be pointed out, however, that an aligned outlet-tube and LAD channel may be impractical in terms of integration inside an actual propellant tank.

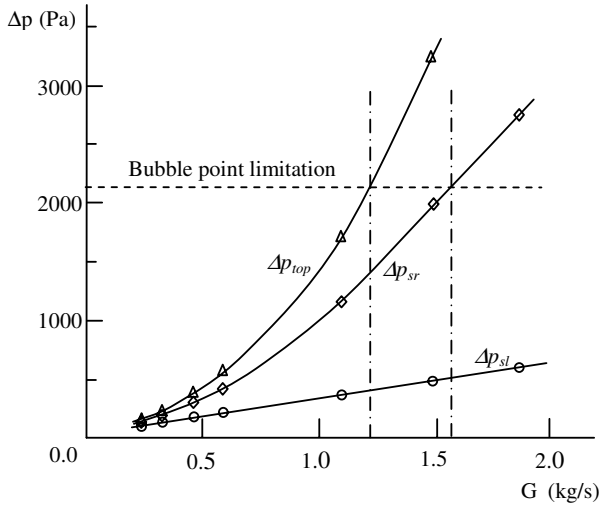

Fig. 9 Three strategic pressure drops in the channel vs. flow rate

II. CONCLUSIONS

The CFD simulation revealed that the flow passing through the screen is continuously augmented along the channel length rather than a uniform flow distribution along the channel length. The outlet-tube position and alignment strongly affect both flow passing through the screen and the flow in the channel. In the configuration that was analyzed, two vortices were created around the entrance of the outlet-tube and produced two low pressure zones that greatly increased the total pressure loss in the assembly.

Because the flow rate in the channel is augmented along the channel length, the flow is subjected to increasing resistance along this length. This flow resistance is neither simple friction resistance nor the resistance created by the change in flow area, it is produced by the flow entering from across the screen impacting and merging with the channel flow. The mathematical expression of the relationship between the resistance Δp_{im} and the working flow rate G has not been developed. More experimental and theory studies are needed.

In order to avoid bubble breakthrough, i.e, the bubble point pressure, the flow rate should not exceed 1.22 kg/s for the current test LAD channel assembly. However, if the vortices around the outlet-tube entrance can be eliminated or reduced by changing the position and alignment of the outlet-tube, the working flow rate limitation would be increased to at least 1.577 kg/s. A combination of using an aligned outlet-tube and a horn-type connection between the channel and the outlet-tube is one method to improve the LAD channel assembly performance.

REFERENCES

[1] D. A. Fester, A. J. Villars, and P. E. Uney, "Surface tension propellant acquisition system technology for space shuttle reaction control tanks," *J. Spacecraft,* vol. 13, No.9, pp. 522-527, 1976,.

[2] M. T. Kudlac, J. M. Jurns, "Screen channel liquid acquisition devices for liquid oxygen," presented at the *42nd AIAA/ASME/SAE/ASEE Joint Propulsion Conference & Exhibit*, Sacramento, CA., July 9-12, 2006, Paper AIAA 2006-5054.

[3] M. V. Dyke, "Identification of influential factors for liquid acquisition device designs," presented at *34th Joint Propulsion Conference and Exhibit*, Cleveland, OH, July 13-15, 1998, Paper AIAA-98-3198.

[4] D. J. Chato, and M. T. Kudlac, "Screen channel liquid acquisition devices for cryogenic propellants," presented at 38th *AIAA/ASME/SAE/ASEE Joint Propulsion Conference & Exhibit*, Indianapolis, IN., July 7-10, 2002, Paper AIAA 2002-3983.

[5] J. M. Jurns, and J. B. McQuillen, "Liquid acquisition device testing with sub-cooled liquid oxygen," presented at 44th *AIAA/ASME/SAE/ASEE Joint Propulsion Conference & Exhibit*, Hartford, CT., July 21-23, 2008, Paper AIAA 2008-4943.

[6] J. C. Armour, and J. N. Cannon, "Fluid flow through woven screens," *Journal AIChE,* vol. 14, No. 3, pp. 415-420, 1968.

[7] E. C. Cady, "Study of thermodynamic vent and screen baffle integration for orbital storage and transfer of liquid hydrogen," NASA-cr-134482, August 1973.